Excitation function studies for deep inelastic processes in $^{19}F+^{27}Al$ collisions

I. Berceanu,[1] A. Andronic,[1] M. Duma,[1] D. Moisă,[1] M. Petrovici,[1] A. Pop,[1] V. Simion,[1] A. Del Zoppo,[2] G. d'Erasmo,[4,5] G. Immé,[2,3] G. Lanzanò,[2,3] A. Pagano,[2,3] A. Pantaleo,[4] and G. Raciti[2,3]

[1]*Institute of Physics and Nuclear Engineering, P.O. Box MG-6, 76900 Bucharest, Romania*

[2]*Istituto Nazionale di Fisica Nucleare, Laboratorio Nazionale del Sud, via Santa Sofia 44, I-95100, Catania, Italy*

[3]*Dipartimento di Fisica, Universita di Catania, I-95129 Catania, Italy*

[4]*Istituto Nazionale di Fisica Nucleare, Sezione di Bari, via Amendola 173, 70125 Bari, Italy*

[5]*Dipartimento di Fisica, Universita di Bari, Italy*

(Received 9 June 1997)

The excitation functions for different fragments produced in the $^{19}F+^{27}Al$ reaction have been measured in the incident energy range 113.5–130.0 MeV in steps of 250 keV. The detection of the outgoing fragments in a large solid angle allowed a study of the excitation functions for different [total kinetic energy loss (TKEL), $\vartheta_{c.m.}$] windows. Large fluctuations have been observed in all the excitation functions analyzed in this work. The Z and angular cross correlation analysis does not support a compound nucleus origin of these fluctuations. The coherence widths extracted from the energy autocorrelation function (EAF) and by the peak counting method do not show, within errors, $\vartheta_{c.m.}$, Z, or TKEL dependence. The lifetime of the dinuclear system (DNS) $^{19}F+^{27}Al$ is found to be equal with the DNS's rotation period. This could explain the secondary structures evidenced in the EAF. A reaction mechanism involving the excitation of the DNS in intermediate states of molecular nature is supported by this experimental evidence. [S0556-2813(98)00105-8]

PACS number(s): 25.70.Lm, 24.60.Ky

I. INTRODUCTION

Experimental studies of the correlations between different observables in $^{19}F+^{27}Al$, $^{19}F+^{12}C$, $^{27}Al+^{27}Al$, and $^{27}Al+^{12}C$ collisions at 111.4, 125.0, 136.9, and 140.1 MeV evidenced that even for such light combinations, in this energy range, a full dynamics specific for deep inelastic processes from quasielastic down to complete damping is present [1–5]. The interaction time extracted from the angular distributions of $Z=9$ fragments for a $^{19}F+^{27}Al$ collision at $E_{lab}=111.4(136.9)$ MeV increases from $\tau_{int}=1.3(0.7)\times10^{-22}$ s to $\tau_{int}=9.4(7.7)\times10^{-22}$ s as the final total kinetic energy (TKE) decreases from the quasielastic towards the complete damping region [1,3]. This shows that these processes cover a wide time scale from fast to slow ones relatively to the passing time value of $\approx5\times10^{-22}$ s.

The experimental evidence of the fluctuations in the excitation function for dissipative heavy ion collisions (DHIC's) [6] allowed the study of the time evolution of the dinuclear system (DNS) formed in the early stage of the collision with a new method, based on statistical analysis [7]. This method was used to study the time evolution of the DNS with different mass asymmetries where the mass of the combined system was lower than 108 [6,8–13]. Strong fluctuations have been evidenced in the excitation functions of the dissipative processes for all these combinations though the extension of Ericson fluctuation theory to DHIC's predicts strong damping with the increasing mass [14]. Their persistence is explained in the framework of the partially overlapping molecular level model (POMLM) [15].

The study of the excitation functions for $^{19}F+^{27}Al$ collision in the energy interval $E_{lab}=113.5-130.0$ MeV reported in the present paper has been performed in order to complete the information on the dinuclear system configuration and its time evolution obtained from our previous measurements [1,3,16]. The experimental device allowed us to study the lifetime dependence of this α-nonconjugate DNS as a function of the charge number Z, emission angle $\vartheta_{c.m.}$, and total kinetic energy loss (TKEL), in contrast with previous works where similar studies have been done integrating on the TKEL.

II. EXPERIMENTAL METHOD

The experiment was performed at the SMP Tandem accelerator from LNS-Catania. Self-supporting ^{27}Al targets of 39 $\mu g/cm^2$ were used. Thus, the energy loss in the target (≈75 keV) was much lower than the energy increment of 250 keV (147 keV in the center of the mass system) used for the excitation function. The beam current was measured with a tantalum-plated Faraday cup provided with an electron-suppressing guard ring.

The outgoing fragments were detected and identified using the experimental device DRACULA [17,18] from which only the large area position sensitive ionization chambers (IC's) and the associated parallel plate avalanche counters in front of them were operated. The IC's were filled with an $Ar(90\%)+CH_4(10\%)$ mixture at 243 torr. The polar and azimuthal angles spanned by the IC's are $\Delta\vartheta=24°$ and $\Delta\varphi=4°$, respectively. The energy resolution at the elastic peak was 2.5%, the angular resolution 0.5°, and the charge resolution better than 0.3 charge units.

Continuous measurements in the angular range from 3° to 54° in the laboratory system (LS) have been previously done for the $^{19}F+^{27}Al$ collision at 111.4, 125, and 136.8 MeV using this experimental setup [1,2]. Based on the representations of the double differential cross section $d^2\sigma/d\text{TKE}\ d\vartheta_{c.m.}$ as a function of $\vartheta_{c.m.}$ and TKE obtained in these measurements, an optimum position of the experimental setup for measuring the excitation function for deep

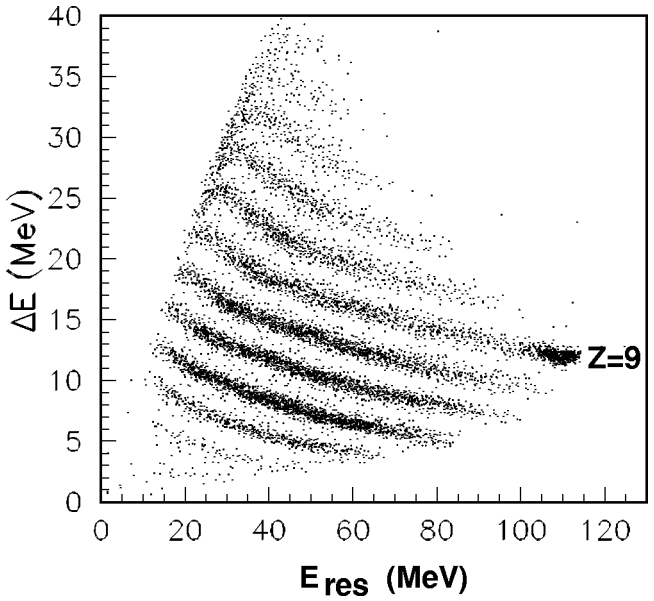

FIG. 1. Identification matrix for the $^{19}F+^{27}Al$ reaction at the incident energy $E_{lab}=120$ MeV.

inelastic processes in $^{19}F+^{27}Al$ collisions has been established. In this experiment the IC's were centered at 27° in the LS to avoid the ridge developed in the Wilczynski plot at angles slightly below the grazing value. Hence the angular range $15° \leqslant \vartheta_{lab} \leqslant 39°$ ($\vartheta_{c.m.} \approx 20° - 70°$) was continuously covered in a single measurement for each incident energy. Consequently, the quasielastic component of the energy spectra is suppressed ($\vartheta_{gr}^{lab}=10.6°$ for the lowest incident energy).

Figure 1 shows an example of a Z identification matrix using one of the possible configurations of the specific energy loss (ΔE) and residual energy (E_{res}). The obtained TKE spectra for $Z=6-12$ fragments are shown in Fig. 2 for one of the bombarding energies, $E_{lab}=125$ MeV. The arrows at low TKE indicate the total kinetic energy corresponding to complete energy dissipation [19]. Small elastic and quasielastic components are present in the energy spectrum of $Z=9$ fragments. Only the dissipated component is present in the energy spectra of the other reaction products. Because of the energy thresholds of the IC's, the energy range corresponding to complete dissipation is covered only for $Z \leqslant 9$ fragments. The energy spectra are corrected for nucleon evaporation using an iterative procedure as described in Ref. [20]. The available excitation energy was shared proportionally with the masses of the two reaction products and a parametrization of the neutron and proton separation energies as a function of the N/Z ratio in the mass region up to 50 has been used [1]. The shape of the corrected TKE spectra is not changed by this correction. However, the most probable total kinetic energies $\langle \mathrm{TKE} \rangle$ shift towards larger energies by 3 – 6 MeV.

III. EXPERIMENTAL RESULTS

A sample of double differential cross sections $d^2\sigma/d\mathrm{TKE}\ d\vartheta_{c.m.}$ for different Z values is given in Fig. 3. In this work are presented the results relative to the excitation functions for the ranges in Z, $\vartheta_{c.m.}$, and TKEL listed in

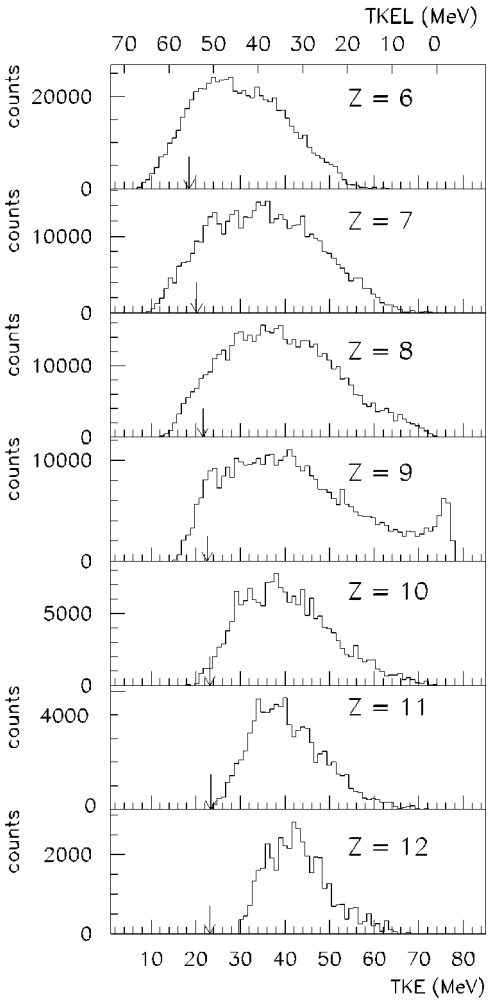

FIG. 2. Total kinetic energy spectra for $Z=6-12$ reaction products in the $^{19}F+^{27}Al$ collision at the bombarding energy $E_{lab}=125$ MeV. The arrows at low TKE values indicate the energy corresponding to fully relaxed processes following the formula of Ref. [19].

Table I. The corresponding windows of the TKEL and $\vartheta_{c.m.}$ can be followed in Fig. 3. The TKEL ranges were chosen to avoid the ridge of the Wilczynski plot corresponding to the complete energy dissipation which is rather well developed for the fragments with $Z \leqslant Z_{proj}$ as can be seen in Fig. 3.

The angular distributions for $Z=6$ and 8 fragments corresponding to the three TKEL windows, at the bombarding energy $E_{lab}=113.5$ MeV, are presented in Figs. 4(a) and 4(b), respectively. Even for this limited angular range one can see the specific trend of DHIC angular distributions, a decreasing slope as a function of the TKEL. The isotropy is reached only for the $Z=6$ reaction fragment for the W5 window which corresponds to the largest energy loss considered in this paper.

The points of an excitation function represent the number of events integrated on a (TKEL, $\vartheta_{c.m.}$) domain for a given Z value normalized to the corresponding collected charge. The excitation functions corresponding to Z values and (TKEL, $\vartheta_{c.m.}$) windows from Table I can be followed in Figs. 5–7. They display fluctuations with amplitudes larger than the statistical errors. A first inspection of these excitation functions shows that (i) the fluctuations persist when changing the

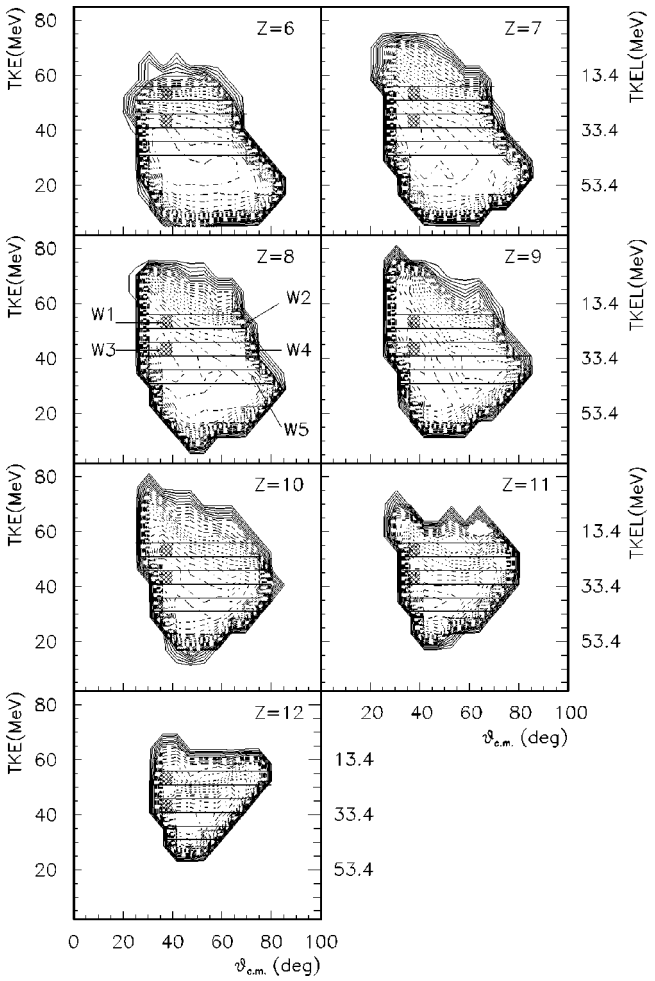

FIG. 3. The (TKEL, $\vartheta_{\mathrm{c.m.}}$) windows for $Z=6-12$ fragments at the incident energy $E_{\mathrm{lab}}=125$ MeV.

TKEL or/and $\vartheta_{\mathrm{c.m.}}$ domains of integration; (ii) for different Z values the fluctuations are strongly correlated, mainly for $Z<Z_{\mathrm{proj}}$.

IV. STATISTICAL ANALYSIS

The fluctuations observed in the excitation functions were studied in the framework of a statistical analysis. In order to establish their nature, the cross correlation coefficients and correlation functions were calculated using general definitions and the results were compared with the predictions given by Ericson fluctuation theory and by approaches developed to describe fluctuation phenomena observed in the excitation functions of DHIC's.

TABLE I. TKEL, $\vartheta_{\mathrm{c.m.}}$, and Z ranges used for the excitation function studies.

	TKEL (MeV)	$\vartheta_{\mathrm{c.m.}}$ (deg)	Z
W1	20 ± 2.5	35–40	6–12
W2	20 ± 2.5	whole range	6–12
W3	30 ± 2.5	35–40	6–12
W4	30 ± 2.5	whole range	6–12
W5	40 ± 2.5	whole range	6–11

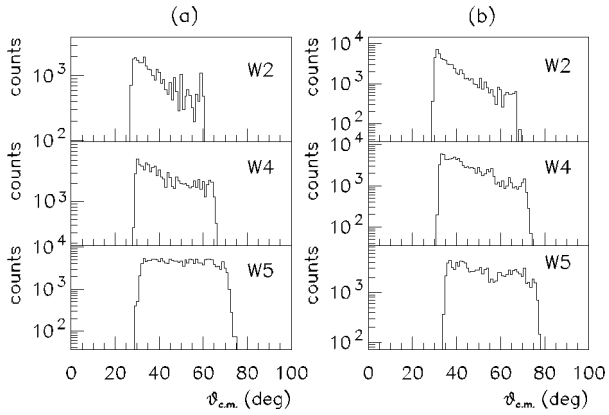

FIG. 4. Angular distributions for (a) $Z=6$ and (b) $Z=8$ reaction products from the $^{19}\mathrm{F}+^{27}\mathrm{Al}$ collision at $E_{\mathrm{lab}}=113.5$ MeV. The values of the W2, W4, and W5 windows are defined in Table I.

A. Cross correlation analysis

The Z and angular cross correlation coefficients have been calculated using the following expression [21]:

$$C_{ij}=\left\langle\left(\frac{\sigma_i(E)}{\overline{\sigma_i(E)}}-1\right)\left(\frac{\sigma_j(E)}{\overline{\sigma_j(E)}}-1\right)\right\rangle[R_i(0)R_j(0)]^{-1/2}, \tag{1}$$

where

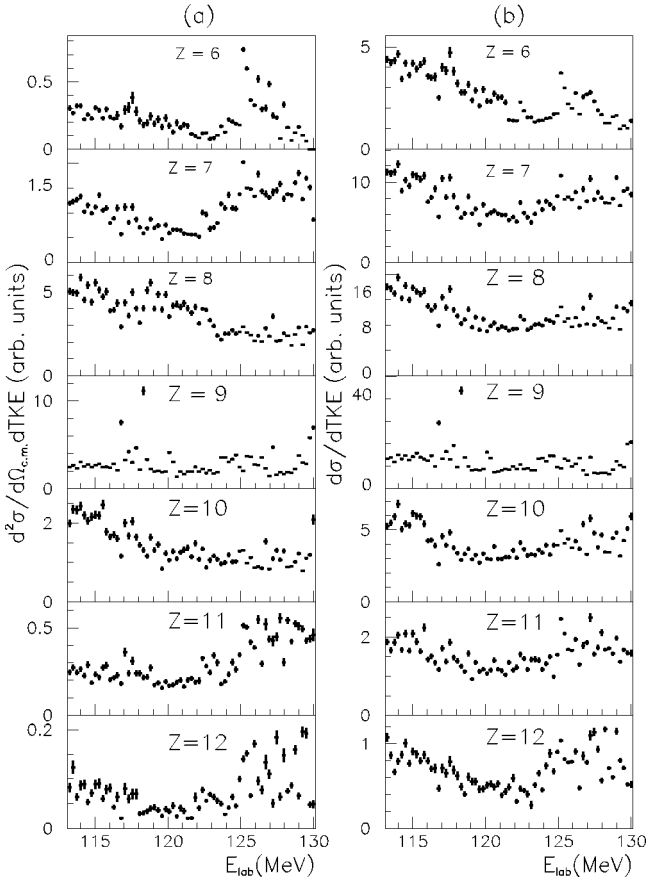

FIG. 5. Excitation functions for $Z=6-12$ fragments for (a) (TKEL, $\vartheta_{\mathrm{c.m.}}$) $\in W1$ and (b) (TKEL, $\vartheta_{\mathrm{c.m.}}$) $\in W2$.

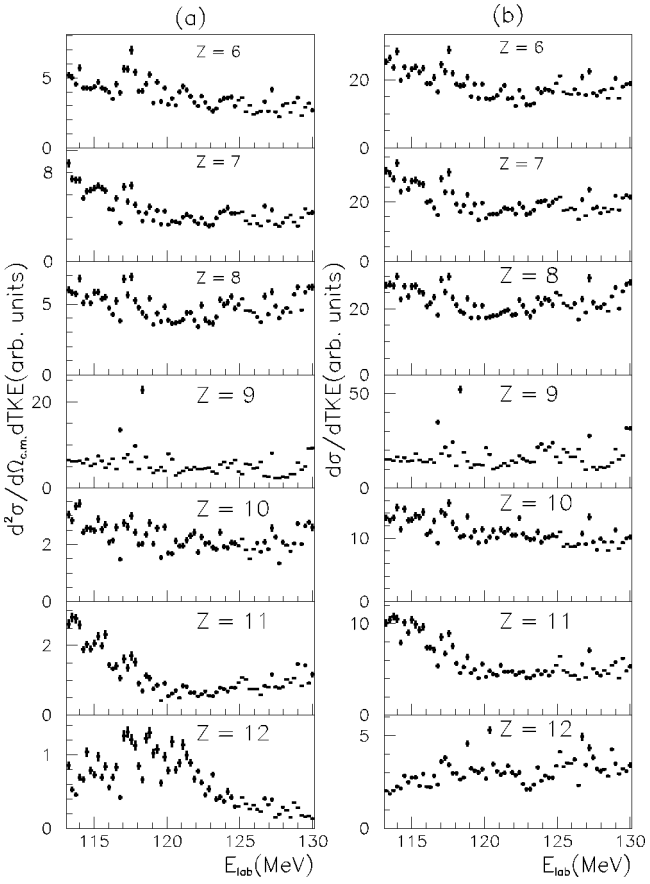

FIG. 6. Excitation functions for $Z=6-12$ fragments for (a) (TKEL, $\vartheta_{\text{c.m.}}) \in W3$ and (b) (TKEL, $\vartheta_{\text{c.m.}}) \in W4$.

$$R_i(0)=\left\langle\left[\left(\frac{\sigma_i(E)}{\overline{\sigma_i(E)}}\right)^2-1\right]\right\rangle.$$

The index $i(j)$ represents Z or $\vartheta_{\text{c.m.}}$, angular brackets represent the average over incoming energy, and $\overline{\sigma_i(E)}$ is the averaged cross section used for removing the gross energy trend of the measured excitation functions. Ericson theory predicts Z cross correlation coefficients equal to zero with some variation due to the finite range of data (FRD) and a small angular coherence width (of the order of $\approx 1/l_{\text{gr}}$, where l_{gr} is the grazing angular momentum and has an average value equal to $48\hbar$ for $^{19}\text{F}+^{27}\text{Al}$ collisions in this energy range) [22].

The values of Z cross correlation coefficients, $C_{Z_1Z_2}$, with FRD errors, for windows W1–W5 are reported in Tables II–VI. The gross energy dependence of the excitation functions was corrected calculating $\overline{\sigma_i(E)}$ as a moving Gaussian average with a width at half maximum of $\Delta_{\text{c.m.}}=2.6$ MeV. The dependence of the $C_{Z_1Z_2}$ values on the averaging interval $\Delta_{\text{c.m.}}$ was studied. A decreasing of the $C_{Z_1Z_2}$ values from 5% to 17% was observed when the $\overline{\sigma_i(E)}$ was calculated using $\Delta_{\text{c.m.}}=4.4$ MeV. For instance, the values 0.59 ± 0.10, 0.75 ± 0.06, 0.61 ± 0.06, 0.48 ± 0.07, and 0.51 ± 0.08 for the C_{6Z_2} ($Z_2=7$, 8, 10 – 12) coefficients were obtained for the W3 window instead of those from the first row of Table IV. Nevertheless, most of the $C_{Z_1Z_2}$ coefficients remain larger than 60% except those for the W1 and W3 windows which are in the vicinity of the geometrical cuts (see the Wilczynski plots in Fig. 3).

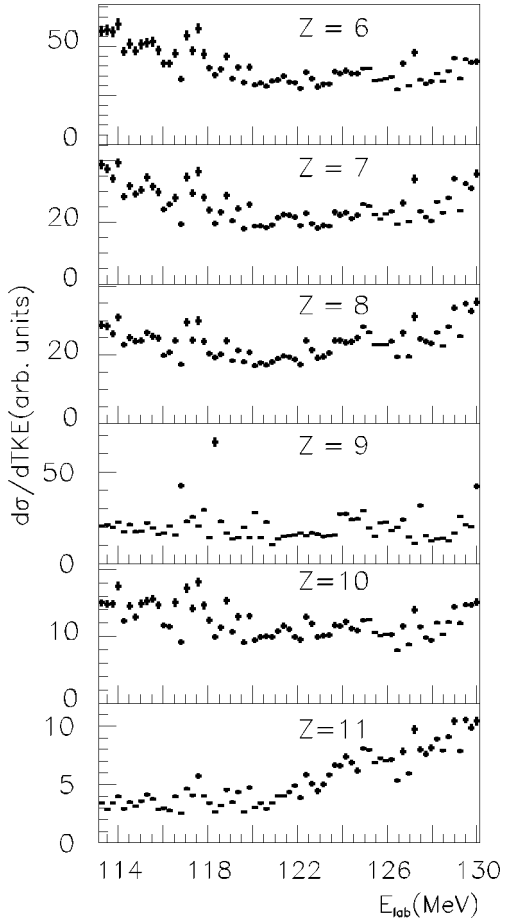

FIG. 7. Excitation functions for $Z=6-11$ fragments for (TKEL, $\vartheta_{\text{c.m.}}) \in$ W5.

For the angular correlation study a set of excitation functions in the bombarding energy range $E_{\text{lab}}=116.75-122.25$ MeV was obtained for the three TKEL ranges given in Table I. The available angular range for $Z=6-8$, 10 fragments was divided in bins of 2°. The values of the angular cross correlation coefficients are large on the whole angular range. Detailed results of this analysis will be published elsewhere.

Based on this cross correlation analysis one can conclude that the fluctuations observed in the present excitation functions are not of compound nucleus origin.

B. Energy autocorrelation function

The energy autocorrelation function (EAF) has been calculated with [22]

TABLE II. Z cross correlation coefficients for the W1 window.

Z	6	7	8	10	11	12
6	1	0.52 ± 0.06	0.16 ± 0.05	0.15 ± 0.10	0.35 ± 0.07	0.35 ± 0.07
7		1	0.28 ± 0.05	0.17 ± 0.05	0.51 ± 0.06	0.75 ± 0.07
8			1	0.42 ± 0.05	0.26 ± 0.06	0.75 ± 0.07
10				1	0.25 ± 0.06	0.14 ± 0.07
11					1	0.39 ± 0.08
12						1

TABLE III. Z cross correlation coefficients for the W2 window.

Z	6	7	8	10	11	12
6	1	0.64±0.06	0.55±0.05	0.51±0.06	0.67±0.07	0.43±0.07
7		1	0.87±0.05	0.76±0.05	0.71±0.06	0.72±0.07
8			1	0.84±0.05	0.69±0.06	0.40±0.07
10				1	0.60±0.06	0.28±0.07
11					1	0.45±0.08
12						1

$$C(\varepsilon)=\left\langle\left(\frac{\sigma(E)}{\overline{\sigma(E)}}-1\right)\left(\frac{\sigma(E+\varepsilon)}{\overline{\sigma(E+\varepsilon)}}-1\right)\right\rangle, \tag{2}$$

where ε is the energy increment in the center of mass system (c.m.s.).

Ericson predicted for the EAF of the excitation functions for the compound nucleus reactions in the region of overlapping resonances a Lorentzian form

$$C(\varepsilon)=\frac{1-y_d^2}{N}\frac{\Gamma^2}{\Gamma^2+\varepsilon^2}, \tag{3}$$

where Γ is the energy correlation width of the fluctuations, y_d the relative contribution of the direct processes to the cross section, and N the number of independent microchannels contributing to the studied excitation function. In [14] a similar expression for the EAF for dissipative processes has been obtained taking into account the correlation between partial waves with different angular momenta. Because of the consideration of the angular momentum coherence, both the EAF and Γ become dependent on the emission angle:

$$C(\varepsilon,\vartheta)=\frac{1}{N}\frac{\Gamma(\vartheta)^2}{\Gamma(\vartheta)^2+\varepsilon^2}. \tag{4}$$

Hence, calculating the experimental EAF using Eq. (2) it is possible to determine the energy correlation width of the fluctuations in the DHIC excitation function using expression (4).

The energy-averaged cross section $\overline{\sigma}(E)$ has been calculated using also a moving Gaussian averaging procedure. An optimum averaging interval $\Delta_{\text{c.m.}}^{\text{opt}}$ was determined investigating the dependence of $C(0)$ on the averaging interval $\Delta_{\text{c.m.}}$ [23]. This is a curve with a plateau reached when $\Delta_{\text{c.m.}}\approx\Gamma$ and which extends until $\Delta_{\text{c.m.}}$ becomes equal with an eventually existing larger energy correlation width. In this region the value of $C(0)$ begins to increase again. The optimum $\Delta_{\text{c.m.}}$ is considered to be the value just before this second increase [23].

TABLE IV. Z cross correlation coefficients for the W3 window.

Z	6	7	8	10	11	12
6	1	0.63±0.06	0.80±0.05	0.64±0.06	0.58±0.07	0.54±0.07
7		1	0.77±0.05	0.64±0.05	0.64±0.06	0.35±0.07
8			1	0.75±0.05	0.66±0.06	0.31±0.07
10				1	0.65±0.06	0.28±0.07
11					1	0.23±0.08
12						1

TABLE V. Z cross correlation coefficients for the W4 window.

Z	6	7	8	10	11	12
6	1	0.87±0.06	0.87±0.05	0.79±0.06	0.80±0.07	0.41±0.07
7		1	0.93±0.05	0.80±0.05	0.84±0.06	0.41±0.07
8			1	0.83±0.05	0.81±0.06	0.38±0.07
10				1	0.76±0.06	0.44±0.07
11					1	0.41±0.08
12						1

Figure 8 shows $C(0)$ versus the averaging interval for the excitation functions corresponding to the W3 window. For $Z=11$ and 12 a second rise of $C(0)$ is well evidenced. For $Z=6$ and 7 such a tendency is less pronounced while for $Z=8$ and 10 the plateau remains even for $\Delta_{\text{c.m.}}$ as large as the whole measured interval (9.7 MeV). The curve corresponding to a Lorentzian fit for the $Z=10$ fragment EAF calculated with $\Delta_{\text{c.m.}}=9.7$ MeV describes quite well the experimental trend as can be seen in Fig. 9(a). The fit of the $Z=8$ fragment EAF calculated with the same value of $\Delta_{\text{c.m.}}$ gives a Γ value of $\approx$400 keV. However, the first points of the EAF ($\varepsilon<1$ MeV) are not very well described by the Lorentzian distribution of this width. For the few cases of this kind the optimum averaging interval was decided taking into account both aspects: the value at which a possible second rise in $C(0)$ appears correlated with the value for which a Lorentzian fit shows a good agreement with the experimental EAF. The arrows in Fig. 8 indicate the optimum $\Delta_{\text{c.m.}}$ determined for each Z value. In this way, in the present analysis only coherence widths for the narrowest fluctuations of the excitation functions were obtained. In fact, for any of the studied excitation functions a second plateau in the representation of the $C(0)$ as a function of $\Delta_{\text{c.m.}}$ was not evidenced. Consequently, it was not possible to evaluate for the observed fluctuations more than one coherence width by this procedure.

The EAF's for the W3 and W4 windows are presented in Figs. 9(a) and 9(b), respectively. The energy averaged cross section $\overline{\sigma}(E)$ was calculated with $\Delta_{\text{c.m.}}^{\text{opt}}$. Similar EAF's were obtained for the W1, W2, and W5 windows. The energy correlation widths Γ were determined by fitting with a Lorentzian form the structure from $\varepsilon=0$ of the EAF's. The dashed lines in Fig. 9 are the result of this fit. The errors in the Γ values were estimated to be $\approx$35%, the statistical, FRD, and gross trend correction contributions being almost equal. In the evaluation of the last contribution it was con-

TABLE VI. Z cross correlation coefficients for the W5 window.

Z	6	7	8	10	11
6	1	0.95±0.05	0.95±0.05	0.93±0.05	0.85±0.05
7		1	0.93±0.05	0.92±0.05	0.83±0.06
8			1	0.94±0.05	0.86±0.05
10				1	0.88±0.06
11					1

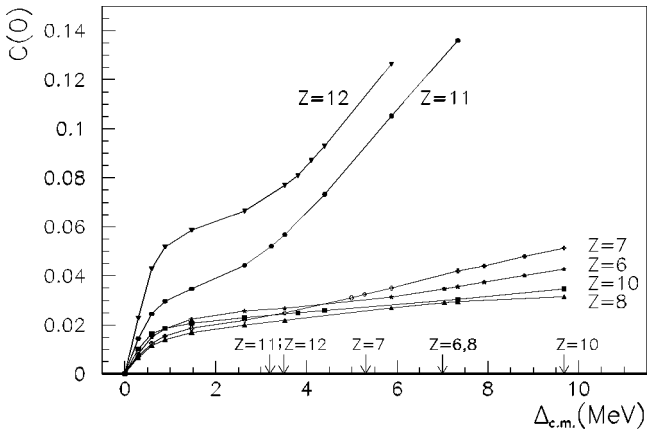

FIG. 8. $C(0)$ as a function of the averaging interval $\Delta_{\text{c.m.}}$ for the excitation functions of the $Z=6-8$, $10-12$ fragments with (TKEL, $\vartheta_{\text{c.m.}}$) $\in$ W3. The arrows indicate the optimum $\Delta_{\text{c.m.}}$ determined following the procedure suggested in Ref. [23] for each excitation function.

sidered that the optimum averaging interval could be estimated with an error of ± 0.295 MeV (c.m.s. energy interval between three experimental points). The Γ values for the windows W1–W5 are represented as a function of Z in Fig. 10(a).

The correlation energies for the W1–W5 windows have been also calculated by the peak counting method (PCM) using the following expression [24]:

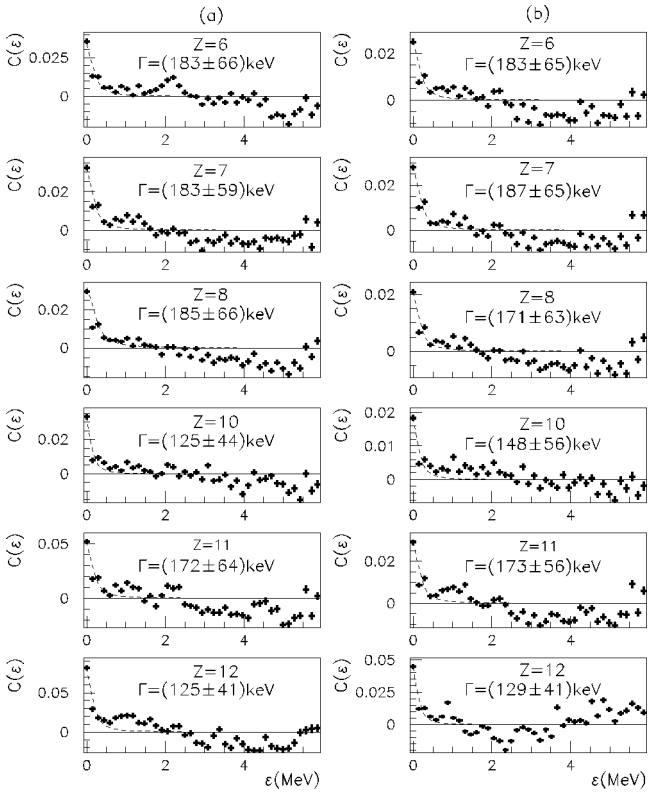

FIG. 9. (a) The EAF for the excitation functions for $Z=6-8$, $10-12$ fragments with (TKEL, $\vartheta_{\text{c.m.}}$) $\in$ W3. (b) The EAF for the excitation functions for $Z=6-8$, $10-12$ fragments with (TKEL, $\vartheta_{\text{c.m.}}$) $\in$ W4. The dashed curves represent the best fit with a Lorentz function of the EAF points with $\varepsilon<1$. The reported errors of the Γ values include the statistical and FRD errors.

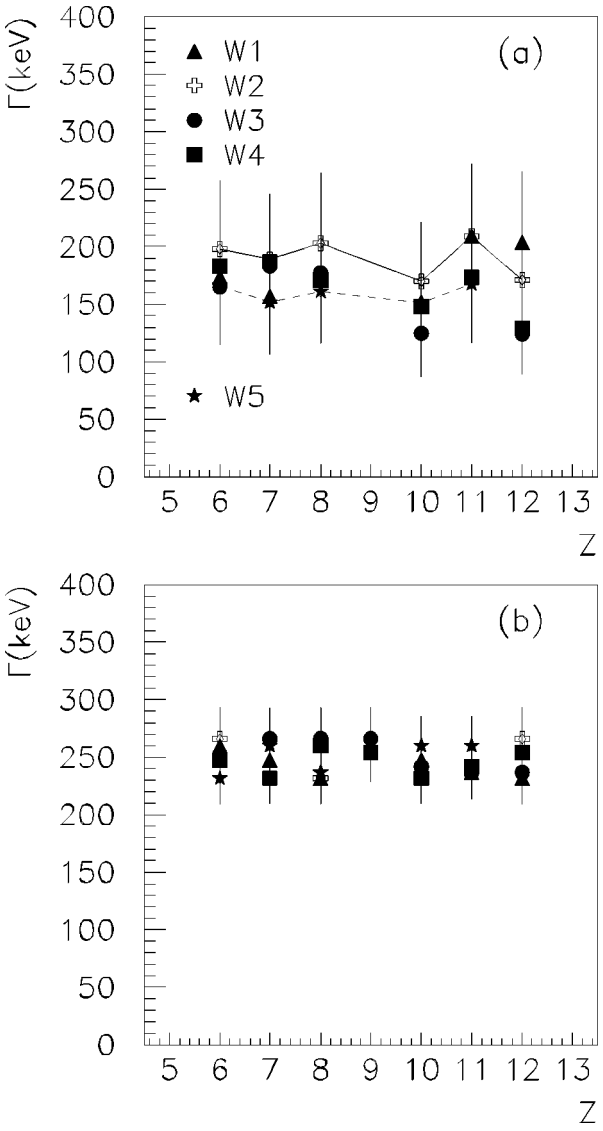

FIG. 10. (a) The coherence energies determined by EAF method as a function of Z for the W1−W5 windows. (b) The coherence energies determined by the PC method as a function of Z for the W1−W5 windows.

$$\Gamma(\text{MeV}) = 0.55/K,$$

where K is the number of peaks per energy unit in the corresponding excitation function. The effect of the number of unresolved microchannels contributing to the studied excitation function was not considered. There are studies which have shown that this effect is smaller [24,25] than initially proposed [26]. The results are presented as a function of Z in Table VII and Fig. 10(b). The FRD errors have been estimated using the result of the synthetic excitation function analysis [25] corresponding to the present number of independent experimental points, $n \approx 45$.

Within the errors, Figs. 10(a) and 10(b) do not show any clear $\vartheta_{\text{c.m.}}$ or Z dependence of the correlation energy as evidenced in Refs. [10,12]. There is no clear evidence of a dependence on the TKEL of the Γ. The Γ values obtained by the PCM are systematically larger than those obtained from the energy autocorrelation function as was already shown [25]. The values of the coherence width obtained by these

TABLE VII. Coherence energies in keV obtained by the peak counting method.

Z	6	7	8	9	10	11	12
W1	260±26	247±25	232±23	254±25	247±25	237±24	232±23
W2	266±27	232±23	232±23	254±25	232±23	242±24	266±27
W3	253±25	266±27	266±27	266±27	242±24	237±24	237±24
W4	247±25	232±23	260±26	254±25	232±23	242±24	254±25
W5	232±23	260±26	237±24	266±27	260±26	260±26	

methods can be considered grouped around the average values $\Gamma_{EAF}=(170\pm65)$ keV and $\Gamma_{PCM}=(248\pm30)$ keV. The corresponding lifetimes of the dinuclear system are $\tau_{EAF}=(3.9\pm1.1)\times10^{-21}$ s and $\tau_{PCM}=(2.6\pm0.2)\times10^{-21}$ s.

Besides the Lorentzian structure at $\varepsilon=0$, the EAF's given in Figs. 9(a) and 9(b) present oscillations with periodicity of ≈1 MeV. The presence of these oscillations in the EAF of the excitation functions for dissipative processes has been predicted taking into account the interference between different revolutions which can occur when the DNS lifetime is larger than the DNS rotation period $T=2\pi/\omega$. The energy period of these oscillations is $\varepsilon_c=\hbar\omega$ [27,28]. The angular velocity of the DNS is given by $\omega=l/\mathcal{J}_{rel}$, where l and $\mathcal{J}_{rel}$ are the angular momentum and moment of inertia in the exit channel, respectively.

The dependence of the ε_c on the moment of inertia allows us to have an estimate for the separation distance of the final fragments at the scission, by comparing the ε_c value with the experimental periodicity. It has been usually obtained from the most probable energies in the final channels, $\langle$TKE$\rangle$ [29,30].

The $\langle$TKE$\rangle$ for the $Z<Z_{proj}$ and $Z=9$ fragments with an error of ±0.5 and ±1.5 MeV, respectively, could be evaluated from the TKE spectra. For $Z>Z_{proj}$ an estimation of $\langle$TKE$\rangle$ was not possible due to the larger energy thresholds of the IC's mentioned before. The $\langle$TKE$\rangle$ values for $Z<Z_{proj}$ fragments present a variation of ≈3 MeV on bombarding energy range. As an example, for the $Z=8$ reaction product the $\langle$TKE$\rangle$ is ≈35 MeV at 113.5 MeV and ≈37.5 MeV at 130 MeV. The separation distances $d=10.7$ and 11.3 fm for $^{16}O+^{30}Si$ fragmentation were obtained from $\langle$TKE$\rangle$ for $E_{lab}=113.5$ and 130.0 MeV, respectively. It was supposed that $\langle$TKE$\rangle$ equals the final channel barrier given by Coulomb and centrifugal energies [29].

The calculated periodicity ε_c can be obtained without considering angular momentum dissipation and in this case l was taken at the middle of the entrance channel angular momentum window, $l=(l_{cr}+l_{gr})/2$ (l_{cr} is the critical angular momentum). For l_{cr} a value of $35.5\hbar$ was estimated using a formula given in Ref. [31]. When the dissipation of the angular momentum is taken into account the angular momentum in the final channel was considered to be the one which corresponds to the sticking configuration, $l_{st}=l(1-\mathcal{J}_{int}/\mathcal{J}_{tot})$, where $\mathcal{J}_{int}$ is the fragment intrinsic momenta of inertia and $\mathcal{J}_{tot}=\mathcal{J}_{int}+\mathcal{J}_{rel}$.

Table VIII reports the ε_c values for the $^{19}F+^{27}Al$ system obtained for the above assumptions relative to the angular momentum and calculating $\mathcal{J}_{rel}$ for two situations: (i) nondeformed fragments in the final channel (lines 1, 4),

$$\mathcal{J}_{rel}=1.044\mu r_0^2(A_1^{1/3}+A_2^{1/3})^2, \quad r_0=1.3, \tag{5}$$

and (ii) deformed fragments in the final channel with separation distances $d=10.7$ and 11.3 fm (lines 2, 5 and 3, 6, respectively),

$$\mathcal{J}_{rel}=1.044\mu d^2. \tag{6}$$

As one can see, the experimental periodicity agrees with calculated ε_c values only when the deformation in the final channel is considered. For this situation the average number of rotations is ≈1. When the deformation of the fragments is not considered the DNS lifetime exceeds a rotation period but the periodicity of the secondary structure is not reproduced anymore.

From Eq. (4) one can conclude that for the deep inelastic processes $C(0)$ (the value of the EAF for $\varepsilon=0$) should give information about the effective number of independent channels, N, contributing to the measured cross section. However, during the analysis of the present experimental information a significant sensitivity of $C(0)$ to the size of the angular range was not observed [compare the values of $C(0)$ for W1(W2) window with those for W3(W4) from Table IX]. One has to note that the $C(0)$ values from Table IX are the least sensitive quantities to the averaging interval from

TABLE VIII. Calculated period of the secondary structures of the EAF.

l $\hbar$	$\mathcal{J}_{rel}$ (10^{-42} MeV s^2)	ω (10^{21} s^{-1})	T (10^{-21} s)	τ_{EAF}/T (rotations)	ε_c (MeV)
$l=42$	6.3	4.2	1.5	2.5	2.78
	12.5	2.1	3.0	1.3	1.4
	13.9	1.9	3.3	1.2	1.3
$l_{st}=30$	6.3	3.0	2.1	1.8	1.95
$l_{st}=35.5$	12.5	1.8	3.5	1.1	1.2
$l_{st}=36.2$	13.9	1.7	3.8	1.0	1.1

TABLE IX. $C(0)$ values for the excitation functions corresponding to the W1–W5 windows and for the excitation functions summed on the W2, W4, and W5 windows.

Z	6	7	8	10	11
W1	0.177	0.043	0.030	0.047	0.055
W2	0.059	0.031	0.025	0.031	0.041
W3	0.035	0.032	0.029	0.033	0.052
W4	0.025	0.028	0.021	0.018	0.029
W5	0.022	0.032	0.024	0.030	0.036
W2+W4+W5	0.022	0.029	0.022	0.023	0.026

the present analysis. In order to get a deeper insight into the effect of enlarging the integration interval on $C(0)$, the summed excitation functions on W2, W3, and W5 were obtained for $Z=6-11$ fragments. The amplitude of the fluctuations are not smeared out in the summed excitation functions. The EAF's for these excitation functions were calculated and the $C(0)$ values are reported in the last row of Table IX. Comparing these values to those corresponding to the W2, W4, and W5 rows one could see that they do not decrease very much when the integration interval increases by a factor of 3. A similar behavior can be observed for the $C(0)$ values calculated for the excitation functions of the $^{19}F+^{89}Y$ system [9]. As an example, the $C(0)$ values obtained for the excitation functions measured at $\vartheta_{lab}=160°$ for $Z=8$, 10, and 11 fragments are 0.0045, 0.0056, and 0.0070, respectively, and the $C(0)$ for the summed excitation function for all these fragments is 0.0041. These aspects agree with the observation that the interpretation of $C(0)$ is not so clear for deep inelastic processes due to the weighting factors which have to be considered for independent states contributing in a given (TKEL, $\vartheta_{c.m.}$) domain [32].

V. DISCUSSION

The DNS lifetime determined in the present work by the EAF method, $\tau_{EAF}=(3.9\pm1.1)\times10^{-21}$ s, is larger than the lifetime extracted from angular distributions for $Z=9$ fragments in the previous studies of deep inelastic processes for $^{19}F(111.4\ MeV)+^{27}Al$ and $^{19}F(136.9\ MeV)+^{27}Al$ collisions [1,3]. For comparison the DNS lifetimes as a function of TKEL obtained in [1,3] for the case of no intrinsic rotation of fragments after separation (τ_{int}) and for the case of a sticking limit (τ_{int}^{st}) are presented in Tables X and XI. The TKEL ranges of the W1 and W3 windows correspond approximately to the second and fourth windows from Table X and to the fourth and sixth windows from Table XI. Similar differences have been reported in Ref. [8] for the $^{19}F+^{89}Y$ system.

The composite system $^{46}_{22}Ti$ studied in this paper was not included in the classification concerning the prediction for the molecular resonance observation in elastic and inelastic scattering in the framework of the orbiting cluster model [33,34]. The nearest system for which such predictions and measurements have been done is the α-like isotope $^{44}_{22}Ti$. Recently, the excitation functions of this composite system for the fusion reaction of $^{12}C+^{32}S$ have been analyzed [35], the coherence energy of 235 ± 31 keV (251 ± 35 keV) being

TABLE X. Lifetimes in 10^{-22} s units extracted from the angular distribution of the $Z=9$ fragments for $^{19}F(111.4MeV)+^{27}Al$ collisions [1].

TKEL (MeV)	39.4–33.4	33.4–27.4	27.4–21.4	21.4–15.4	15.4–9.4
τ_{int}	4.3	3.1	0.8	0.7	0.6
τ_{int}^{st}	9.4	6.8	1.8	1.5	1.3

determined for a 110 keV (220 keV) energy increment using the spectral density method (SDM). The Γ values obtained in the present work are in good agreement with these data considering that the SDM gives larger values of Γ than the EAF.

A summary of the Γ values as a function of Z for DHIC's is presented in Fig. 11. The bombarding energy range and ϑ_{gr} corresponding to the lowest incident energy are mentioned for every system. In Fig. 11(a) are represented, for simplicity, the Γ values obtained for the $^{19}F+^{27}Al$ system using the EAF for W2 and W5 windows. One can see that the measurement of the excitation function for the $^{19}F+^{27}Al$ system is done on the largest energy interval. This allowed us to obtain cross correlation coefficients and Γ values with small FRD errors. The data obtained from the $^{12}C+^{24}Mg$ collision excitation function measured on an incident energy interval larger than those for the systems presented in Figs. 11(b)–11(f) are not included in this figure because the observed fluctuations wash out when one integrates on the TKEL [8,32].

One could see that Γ values for the $^{19}F+^{27}Al$ system agree better with the values for other systems when they are obtained using the same method. The SDM always gives larger Γ values relative to the ones obtained by the EAF procedure [see Figs. 11(b), 11(c)]. The data for the $^{19}F+^{89}Y$ system from Ref. [9] have been analyzed by the SDM in Ref. [10].

As was mentioned before, the Γ values reported in the present work do not show $\vartheta_{c.m.}$ or Z dependence. The Γ values reported for the other systems, except that obtained by the EAF method for $^{19}F+^{89}Y$, show a clear dependence on Z and/or the observation angle. One possible explanation of the different pattern of the Γ values as a function of Z for the $^{19}F+^{27}Al$ system could be the fact that the present measurement was done at angles larger than the grazing angle, while in the cases where a pronounced Z dependence was evidenced the observation angle was smaller than the grazing angle ($^{28}Si+^{64}Ni$ and $^{28}Si+^{48}Ti$ systems). Another explanation could be that for the systems from Figs. 11(b)–11(f) the excitation functions have been obtained integrating over the whole range of the TKEL. In the present study the contribution from the quasielastic component is almost excluded. The contribution of the quasielastic events not excluded for systems from Figs. 11(b), 11(d)–11(f) could produce a Γ dependence of this pattern, namely, larger Γ values for reaction products having atomic numbers near Z_{proj}. The authors of these papers introduced contributions from a fast and slow mechanism in different ratios, determined on the basis of the angular distribution analysis, to explain the observed pattern of Γ as a function of Z. For the $^{19}F+^{89}Y$ system the excitation functions for $\vartheta_{lab}=60°$, 120°, and 160° have been measured. The Γ values obtained by the EAF method [9] do not

TABLE XI. Lifetimes in 10^{-22} s units extracted from the angular distribution of the $Z=9$ fragments for ^{19}F(136.9 MeV)+^{27}Al collisions [3].

TKEL (MeV)	54.4–48.4	48.4–42.4	42.4–36.4	36.4–30.4	30.4–24.4	24.4–18.4
τ_{int}	3.5	2.2	1.7	1.2	0.9	0.7
τ_{int}^{st}	7.7	4.8	3.8	2.6	2.0	1.5

present an angular dependence and the Z dependence is very weak as can be seen from Fig. 11(c). Only for the data analyzed by the SDM has the Z dependence been evidenced.

The analysis of the excitation functions for different TKEL values was started with the idea to evidence a TKEL dependence of the Γ values. However, such a dependence was not found in the considered TKEL range. Before concluding that the EAF method is not sensitive to the TKEL, studies on larger TKEL ranges are required. This is supported by the observation that the Γ values for the lowest TKEL window W2 are larger than those for the largest TKEL value W5 for all Z fragments as can be seen in Fig. 10(a) where with a solid (dashed) line are connected the Γ values for the W2 (W5) window.

Recently, a unified description of the fluctuation phenomenon in the elastic, inelastic, and dissipative collisions of

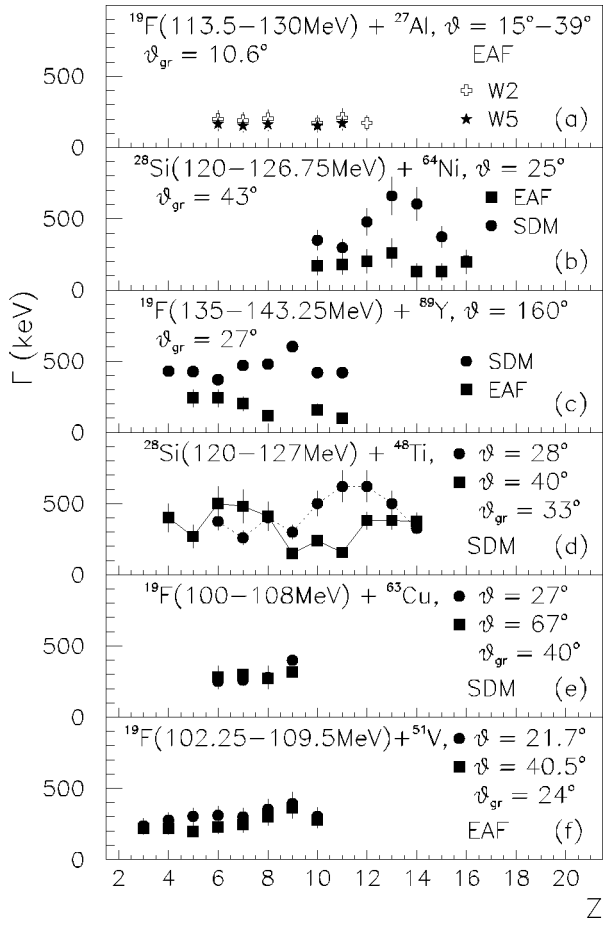

FIG. 11. The comparison of coherence energies obtained for DHIC's in the ^{19}F+^{27}Al system with the coherence energies for dissipative processes in other systems: (a) present work; (b), (c), (d), (e), (f) data from Refs. [6,9–11,36], respectively. The angles are in the LS, except for panel (d) where they are in the c.m.s.

light heavy ions has been realized in the framework of the POMLM [15]. The POMLM was based on the observation that for dissipative heavy ion collisions in the energy range 5–10 MeV/nucleon the entry region of the excitation of the DNS in the $(E_{c.m.},l)$ plane is near the yrast line. The Ericson formalism condition $\Gamma \gg D$ (totally overlapped states) is relaxed to $\Gamma \geqslant (1-30)D$ which does not destroy completely the correlation between the final channels.

In order to explain the large correlation between different final states observed in DHIC's, the hypothesis has been advanced that only a few special final states are selectively populated and these can decay by equilibrium or preequilibrium light particle or gamma ray emission [37]. Measurements of gamma rays in coincidence with projectilelike fragments (PLF's) showed a statistical deexcitation of the fragments emitted in the DHIC's ^{28}Si, and ^{32}S+^{64}Ni at 5 MeV/nucleon [37]. Nonstatistical gamma rays have been found to be emitted in coincidence with PLF's from quasielastic ^{28}Si+^{64}Ni collisions at 143 MeV [38]. This experimental evidence gives support to the POMLM hypothesis that the reduced amplitudes are random variables with a Gaussian distribution.

The entry region of the DNS ^{19}F+^{27}Al in the present experiment is a few MeV above the calculated yrast line using the formula of Ref. [33]. The fluctuations observed in the excitation functions for dissipative processes in ^{19}F +^{27}Al collisions could be due to the excitation of the DNS in the low density region of the rotational states. The results of the statistical analysis for the excitation functions, the large cross correlation coefficients for channels with different Z numbers, the large angular cross correlation coefficients, and the pattern of the Γ values as a function of Z are described qualitatively in the framework of the POMLM.

VI. CONCLUSIONS

The measurements of ^{19}F+^{27}Al collisions in the energy interval 113.5–130.0 MeV with detection of the outgoing fragments in a large solid angle and energy range allowed us to study the excitation functions of the fragments with atomic number $Z=6-12$ for different (TKEL, $\vartheta_{c.m.}$) domains. Large fluctuations are present in all considered excitation functions. The Z and angular cross correlation analysis shows that these fluctuations are not of compound nucleus origin. The coherence energies obtained by the energy autocorrelation function and peak counting method do not show, within the errors, a $\vartheta_{c.m.}$, Z, or TKEL dependence. The lifetime of the ^{19}F+^{27}Al DNS extracted from the coherence width is equal to a DNS rotation period which could explain the secondary structures evidenced in the EAF. Interpreting

the secondary structures in the EAF as due to the interference between different revolutions, the agreement between the experimental oscillation and calculated periodicity is obtained considering deformed fragments in the final channel.

Experimental evidence from the present work supports the idea of a reaction mechanism involving the excitation of the DNS in intermediate states of molecular nature as proposed by the POMLM [15].

ACKNOWLEDGMENTS

We are grateful to the technical staff of the different institutes and to the LNS-Catania SMP accelerator crew for the quality of the delivered beam. For the high quality targets used during the experiment we own the special knowledge of C. Marchetta. Special thanks are due to Prof. G. Pappalardo and Dr. M. Papa for detailed discussions and suggestions related to the presented topics.

[1] M. Petrovici, A. Andronic, I. Berceanu, A. Buţă, M. Duma, D. Moisă, A. Pop, V. Simion, A. Bonasera, G. Immé, G. Lanzanò, A. Pagano, G. Raciti, N. Colonna, G. d'Erasmo, and A. Pantaleo, Z. Phys. A **354**, 11 (1996).

[2] M. Petrovici, A. Andronic, I. Berceanu, A. Buţă, M. Duma, D. Moisă, A. Pop, V. Simion, A. Bonasera, G. Immé, G. Lanzanò, A. Pagano, G. Raciti, N. Colonna, G. d'Erasmo, and A. Pantaleo, INFN-LNS Activity Report 1993–1995, Catania, 1996, p. 18.

[3] M. Petrovici, A. Andronic, I. Berceanu, A. Buţă, M. Duma, D. Moisă, A. Pop, V. Simion, A. Bonasera, G. Immé, G. Lanzanó, A. Pagano, G. Raciti, N. Colonna, G. d'Erasmo, and A. Pantaleo, INFN-LNS Activity Report 1993–1995, Catania, 1996, p. 27.

[4] A. Pop, A. Andronic, I. Berceanu, A. Buţă, M. Duma, D. Moisă, M. Petrovici, V. Simion, A. Bonasera, G. Immé, G. Lanzanò, A. Pagano, G. Raciti, N. Colonna, G. d'Erasmo, and A. Pantaleo, Phys. Lett. B **397**, 25 (1997).

[5] A. Pop, A. Andronic, I. Berceanu, A. Buţă, M. Duma, D. Moisă, M. Petrovici, V. Simion, A. Bonasera, G. Immé, G. Lanzanò, A. Pagano, G. Raciti, R. Coniglione, A. Del Zoppo, P. Piatelli, P. Sapienza, N. Colonna, G. d'Erasmo, and A. Pantaleo, Abstracts of the European Conference on Nuclear Physics, Thessaloniki, 1997, p. 113.

[6] A. De Rosa, G. Inglima, V. Russo, M. Sandolini, G. Fortuna, G. Montagnoli, C. Signorini, A. M. Stefanini, G. Cardella, G. Pappalardo, and F. Rizzo, Phys. Lett. **160B**, 239 (1985).

[7] T. Ericson and T. Mayer-Kuckuk, Annu. Rev. Nucl. Sci. **16**, 183 (1966).

[8] A. Glaesner, W. Dünnweber, W. Hering, D. Konnerth, R. Ritzka, R. Singh, and W. Trombik, Phys. Lett. **169B**, 153 (1986).

[9] T. Suomijärvi, B. Berthier, R. Lucas, M. C. Mermaz, J. P. Coffin, G. Guillaume, B. Heusch, F. Jundt, and F. Rami, Phys. Rev. C **36**, 181 (1987).

[10] A. De Rosa, G. Inglima, M. Romano, V. Russo, M. Sandolini, G. Cardella, G. Pappalardo, F. Rizzo, G. Fortuna, A. M. Stefanini, S. Beghini, G. Montagnoli, and C. Signorini, Phys. Rev. C **37**, 1042 (1988).

[11] G. Cardella, M. Papa, G. Pappalardo, F. Rizzo, Q. Wang, A. De Rosa, E. Fioretto, G. Inglima, M. Romoli, M. Sandoli, R. Setola, L. Corradi, G. Montagnoli, and A. M. Stefanini, Z. Phys. A **336**, 387 (1990).

[12] F. Rizzo, G. Cardella, A. De Rosa, A. Di Pietro, A. D'Onofrio, E. Fioretto, G. Inglima, M. Papa, G. Pappalardo, M. Romano, M. Romoli, F. Terrasi, M. Sandoli, and G. S. Wang, Z. Phys. A **349**, 169 (1994).

[13] M. Papa, G. Cardella, A. Di Pietro, S. L. Li, A. Musumarra, G. Pappalardo, F. Rizzo, A. De Rosa, G. Inglima, M. La Comarra, D. Pierroutsakou, and M. Romoli, Z. Phys. A **353**, 205 (1995).

[14] D. M. Brink and K. Dietrich, Z. Phys. A **326**, 7 (1987).

[15] M. Papa, Ph.D. thesis, VI Cycle, Catania University, 1994.

[16] I. Berceanu, A. Andronic, M. Duma, D. Moisă, M. Petrovici, A. Pop, V. Simion, G. d'Erasmo, A. Del Zoppo, G. Immé, G. Lanzanò, A. Pagano, A. Pantaleo, and G. Raciti, Abstracts of the European Conference on Nuclear Physics, Thessaloniki, 1997, p. 10.

[17] M. Petrovici, V. Simion, I. Berceanu, A. Demian, M. Duma, M. Ivaşcu, D. Moisă, E. Osvath, G. Pascovici, R. Bock, A. Gobbi, K. D. Hildenbrand, U. Lynen, H. Sann, G. Augustinski, H. Beeskov, and H. W. Daues, IPNE Report No. NP-55-1986, 1986.

[18] V. Simion, Rom. J. Phys. **38**, 513 (1993).

[19] V. E. Viola, K. Kwiatkowski, and M. Walker, Phys. Rev. C **31**, 1550 (1985).

[20] H. Breuer, N. R. Yoder, A. C. Mignerey, V. E. Viola, K. Kwiatkowsky, and K. L. Wolf, Nucl. Instrum. Methods Phys. Res. **204**, 419 (1983).

[21] L. C. Dennis, S. T. Thornton, and K. R. Cordell, Phys. Rev. C **19**, 777 (1979).

[22] A. Richter, in *Nuclear Spectroscopy and Reactions*, edited by J. Cerny (Academic, New York, 1974), Vol. B, p. 343.

[23] G. Pappalardo, Phys. Lett. **13**, 320 (1964).

[24] P. J. Dallimore and I. Hall, Phys. Lett. **18**, 138 (1965).

[25] A. Van der Woude, Nucl. Phys. **80**, 14 (1966).

[26] D. M. Brink and O. Stephen, Phys. Lett. **5**, 14 (1963).

[27] Yu. S. Kun, Phys. Lett. B **257**, 247 (1991).

[28] Yu. S. Kun, W. Nörenberg, and M. Papa, Phys. Lett. B **298**, 273 (1993).

[29] C. K. Gelbke, P. Braun-Munzinger, J. Barette, B. Zeidman, M. J. Levine, A. Gamp, H. L. Harney, and Th. Walcher, Nucl. Phys. **A269**, 460 (1976).

[30] J. B. Natowitz, M. N. Namboodiri, R. Eggers, P. Gonthier, K. Geofferoy, R. Hanus, C. Towsley, and K. Das, Nucl. Phys. **A277**, 477 (1977).

[31] W. W. Wilck, J. R. Birkelund, A. D. Hoover, J. R. Huizenga, W. U. Schröder, and H. J. Wollersheim, Report No. UR-NSRL-221, 1980.

[32] A. Glaesner, W. Dünnweber, M. Bantel, W. Hering, D. Konnerth, R. Ritzka, W. Trautmann, W. Trombik, and W. Zipper, Nucl. Phys. **A509**, 331 (1990).

[33] N. Cindro, Ann. Phys. (N.Y.) **13**, 289 (1988).

[34] U. Abbondanno, Phys. Rev. C **43**, 1484 (1987).

[35] M. Lattuada, D. Vinciguerra, C. M. Sutera, G. Inglima, and M.

Sandoli, Phys. Rev. C **35**, 818 (1987).

[36] Wang Qi, Lu Jun, Xu Hushan, Li Songlin, Zhu Yongtai, Fan Enjie, Yin Xu, Zhang Yuhu, Li Zhichang, Zhao Kui, Lu Xiuqin, and Hu Xiaoqing, Phys. Lett. B **388**, 462 (1996).

[37] C. Agodi, R. Alba, A. Anzalone, G. Bellia, G. Cardella, S. Cavallaro, R. Coniglione, A. Del Zoppo, P. Finocchiaro, C. Maiolino, E. Migneco, M. Papa, G. Papplardo, P. Piatelli, F. Rizzo, G. Russo, P. Sapienza, Q. Wang, G. S. Wang, E. Fioretto, G. Inglima, M. Romoli, and M. Sandoli, Z. Phys. A **340**, 341 (1991).

[38] C. Agodi, R. Alba, G. Bellia, A. Bonasera, G. Cardella, R. Coniglione, A. Del Zoppo, A. De Rosa, P. Finocchiaro, E. Fioretto, F. Gulminelli, G. Inglima, M. Longo, C. Maiolino, E. Migneco, M. Papa, G. Papplardo, P. Piatelli, F. Rizzo, M. Romoli, G. Russo, M. Sandoli, and P. Sapienza, Phys. Lett. B **308**, 220 (1993).